A potent cytotoxic photoactivated platinum complex

A potent cytotoxic photoactivated platinum complex

Fiona S. Mackay*, Julie A. Woods[†‡], Pavla Heringová[§], Jana Kašpárková[§], Ana M. Pizarro*[¶], Stephen A. Moggach*, Simon Parsons*, Viktor Brabec[§‡], and Peter J. Sadler*[‡¶]

*School of Chemistry, University of Edinburgh, West Mains Road, Edinburgh EH9 3JJ, United Kingdom; [†]Photobiology Unit, Department of Dermatology, University of Dundee, Ninewells Hospital and Medical School, Dundee DD1 9SY, United Kingdom; [§]Institute of Biophysics, Academy of Sciences of the Czech Republic, Královopolská 135, CZ-61265 Brno, Czech Republic; and [¶]Department of Chemistry, University of Warwick, Gibbet Hill Road, Coventry CV4 7AL, United Kingdom

Edited by Joan Selverstone Valentine, University of California, Los Angeles, CA, and approved November 6, 2007 (received for review August 17, 2007)

We show by x-ray crystallography that the complex *trans*, *trans*, *trans*-[Pt(N$_3$)$_2$(OH)$_2$(NH$_3$)(py)] (1) contains an octahedral Pt^{IV} center with almost linear azido ligands. Complex 1 is remarkably stable in the dark, even in the presence of cellular reducing agents such as glutathione, but readily undergoes photoinduced ligand substitution and photoreduction reactions. When 1 is photoactivated in cells, it is highly toxic: 13–80 x more cytotoxic than the Pt^{II} anticancer drug cisplatin, and *ca.* 15 x more cytotoxic toward cisplatin-resistant human ovarian cancer cells. Cisplatin targets DNA, and DNA platination levels induced in HaCaT skin cells by 1 were similar to those of cisplatin. However, cisplatin forms mainly intrastrand *cis* diguanine cross-links on DNA between neighboring nucleotides, whereas photoactivated complex 1 rapidly forms unusual *trans* azido/guanine, and then *trans* diguanine Pt^{II} adducts, which are probably mainly intrastrand cross-links between two guanines separated by a third base. DNA interstrand and DNA–protein cross-links were also detected. Importantly, DNA repair synthesis on plasmid DNA platinated by photoactivated 1 was markedly lower than for cisplatin or its isomer transplatin (an inactive complex). Single-cell electrophoresis experiments also demonstrated that the DNA damage is different from that induced by cisplatin or transplatin. Cell death is not solely dependent on activation of the caspase 3 pathway, and, in contrast to cisplatin, p53 protein did not accumulate in cells after photosensitization of 1. The *trans* diazido Pt^{IV} complex 1 therefore has remarkable properties and is a candidate for use in photoactivated cancer chemotherapy.

cytotoxicity | DNA binding | photochemistry | cisplatin

Traditional platinum-based anticancer compounds are a clinically successful group of therapeutic agents; however, their use is constrained by dose-limiting side-effects and the problem of acquired resistance (1). To avoid these problems, we are exploring the use of inert, nontoxic platinum complexes that can be activated locally in cancer cells with light (2). In general, photoactivation offers potential for initiating unusual ligand substitution and redox reactions of transition metal complexes (3, 4), and hence photoactivation may offer new mechanisms of anticancer activity.

The light-activated Pt^{IV} complex described here is effective in killing human cancer cells, including cisplatin-resistant cells, but only upon irradiation, thus combining the potent cytotoxic ability of platinum compounds with the selectivity of a light-activated drug. Photodynamic therapy (PDT) uses photosensitizers such as porphyrins, which require oxygen to kill cancer cells via the formation of singlet oxygen. This can be a problem due to the hypoxic nature of many malignant and most aggressive tumors (5); therefore, photoactivatable complexes that do not require oxygen may be more effective. Light-activated drugs are routinely used in treatment of nonmelanoma skin cancers and benign hyperproliferative diseases of the skin, as well as tumors of the brain, lung, esophagus, bladder, pancreas, and bile duct (6).

Platinum(IV) diazido complexes containing *cis*-diam(m)ine ligands are relatively inert in the dark, even in the presence of millimolar concentrations of the intracellular reducing agent glutathione (7–9). We report here the dramatic effects arising from incorporation of a π-acceptor pyridine ligand in place of an ammine ligand. *Trans*, *trans*, *trans*-[Pt(N$_3$)$_2$(OH)$_2$(NH$_3$)(py)] (**1**) is highly phototoxic and reacts with guanine derivatives and with DNA to give unusual Pt^{II} adducts not readily formed in the absence of light.

Results

Stability and Photochemistry. The all-*trans* geometry of **1** determined by x-ray crystallography is shown in Fig. 1. The extensive hydrogen bonding network in the crystals is shown in supporting information (SI) Fig. 5. Complex **1** (or ^{15}N-**1**, 3 mM) was very stable in water and did not react with 5′ GMP (2 mol equiv) in the absence of light over a period of >5 months as judged by NMR spectroscopy. Complex **1** was also relatively stable to reduced glutathione (2 mol equiv), with only ≈5% of Pt^{IV} reduced to Pt^{II} after 21 d.

UVA irradiation (365 nm) of an aqueous solution of **1** gave a decrease in intensity of the azide-to-Pt^{IV} charge-transfer band at 289 nm (Fig. 2*A*), indicating loss of the Pt^{IV}–azide bonds.

After irradiation of an aqueous solution of ^{15}N–**1**, very little reduction to Pt^{II} was observed by 1D ^{1}H and 2D [^{1}H,^{15}N] HSQC NMR spectroscopy. Two of the Pt^{IV} photoproducts were identified as the tetrahydroxy complex *trans*-[Pt(OH)$_4$(^{15}NH$_3$)(py)] (**2**) and the monoazide-trihydroxy complex *trans*-[Pt(N$_3$)(OH)$_3$(^{15}NH$_3$)(py)] (**3**) (SI Fig. 6). Neither 1D ^{1}H nor 2D [^{1}H,^{1}H] COSY NMR spectroscopy gave evidence for release of pyridine from the platinum center. However, subsequent work showed that the presence of nucleophilic biomolecules has a major influence on the photoreaction pathways.

After only 1 min of UVA irradiation of ^{15}N-**1** in the presence of 2 mol equiv 5′-GMP, a new 2D [^{1}H,^{15}N] HSQC NMR peak for a Pt^{II} species (**4**) appeared (Fig. 2*B*). Further irradiation led to the appearance of another new Pt^{II} peak (**5**). The Pt^{II} peaks were assigned as (*SP*-4-4)-[Pt(N$_3$)(^{15}NH$_3$)(py)(5′-GMP)]$^+$ (**4**) δ(^{1}H,^{15}N) 4.15, −66.37, and *trans*-[Pt(^{15}NH$_3$)(py)(5′-GMP)$_2$]$^{2+}$ (**5**) δ(^{1}H,^{15}N) 4.42, −65.63 (confirmed by their synthesis, see *SI Text*). The peak for **4** decreased in intensity upon further

Author contributions: F.S.M., J.A.W., V.B., and P.J.S. designed research; F.S.M., J.A.W., P.H., J.K., and S.A.M. performed research; A.M.P. and S.P. contributed new reagents/analytic tools; F.S.M., J.A.W., P.H., J.K., A.M.P., S.A.M., S.P., V.B., and P.J.S. analyzed data; and F.S.M., J.A.W., J.K., S.P., V.B., and P.J.S. wrote the paper.

Conflict of interest: The University of Edinburgh has filed a patent application relating to complex **1**.

This article is a PNAS Direct Submission.

Freely available online through the PNAS open access option.

Data deposition: The atomic coordinates have been deposited in the Cambridge Structural Database, Cambridge Crystallographic Data Centre, Cambridge CB2 1EZ, United Kingdom (CSD reference no. 646–178). The x-ray crystallographic data for complex **1** can be found in SI published on the PNAS web site.

[‡]To whom correspondence may be addressed. E-mail: j.woods@dundee.ac.uk, brabec@ibp.cz, or p.j.sadler@warwick.ac.uk.

This article contains supporting information online at www.pnas.org/cgi/content/full/0707742105/DC1.

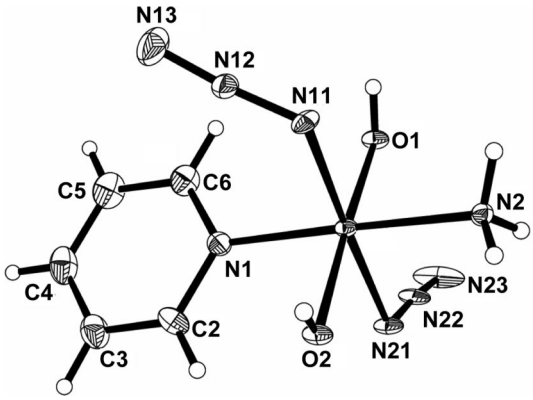

Fig. 1. X-ray crystal structure of **1**. Selected bond lengths (Å) and angles (°): Pt-N(1) 2.059(4); Pt-N(2) 2.020(4); Pt-N(3) 2.044(3); Pt-N(21) 2.046(3); N(11)–N(12) 1.203(5); N(12)–N(13) 1.139(6); N(21)–N(22) 1.216(5); N(22)–N(23) 1.138(5); N(11)–N(12)–N(13) 174.4(5); N(21)–N(22)–N(23) 175.9(5).

irradiation, consistent with light-induced loss of the second azido ligand, whereas the concentration of the *bis*-GMP adduct **5** increased (Fig. 2*C*). Platinum binding to N7 of 5′-GMP was confirmed both by the low-field ^{1}H NMR shift of H8 (10), and by a ^{1}H NMR pH titration (absence of H8 chemical shift change associated with N7 protonation, $pK_a \approx 2.5$ (11) for both Pt^{II} photoproducts **4** and **5**, SI Fig. 7).

Remarkably, the photoreaction with ^{15}N-**1** and 5′-GMP was also induced by red laser light (647.1 nm) despite the low power (≈15 mW), and very low absorbance at this wavelength ($\varepsilon_{647} < 10\ M^{-1}cm^{-1}$; SI Fig. 8). Peaks corresponding to both **4** and **5** appeared after 2.5 h of irradiation.

Phototoxicity. Complex **1** reduced the viability of HaCaT keratinocytes, cisplatin-sensitive A2780, and cisplatin-resistant A2780cis human ovarian carcinoma cells in a dose-dependent manner when photoactivated with UVA (Fig. 3 and Table 1), but was not cytotoxic to HaCaT or A2780cis cells in the dark. A2780 cells were 80-fold more sensitive to photoactivated **1** compared with cisplatin under identical conditions, followed by keratinocytes (24-fold) and A2780cis cells (15-fold). Cisplatin itself showed no difference in potency regardless of whether it was irradiated. Complex **1** was also photoactive in SH-SY5Y neuroblastoma cells (IC_{50} +UVA: 2.4 μM; IC_{50} −UVA: 244 μM; data not shown).

When irradiated with visible light (λ_{max} 420 nm), the complex was as potent as cisplatin under similar conditions (IC_{50} **1** + 5 J/cm^2 TL03: 85.8 μM; Fig. 3*D*), despite very weak absorption by **1** in this part of the spectrum.

DNA Damage in Cells. When HaCaT cells were exposed to 5 J/cm^2 UVA, DNA damage, as measured by migration of DNA from the nucleus in the single cell gel electrophoresis assay, did not change compared with an unirradiated control (2.5 ± 0.4% and 3.1 ± 0.2% DNA in comet tail, respectively). Pretreatment with cisplatin significantly inhibited HaCaT cell DNA migration after H_2O_2 treatment in a dose-dependent manner by a maximum of ≈60% (SI Fig. 9). Transplatin also inhibited DNA migration, but was not cytotoxic to HaCaT cells under these conditions (data not shown).

When complex **1** was photoactivated, a similar dose-dependent decrease in DNA migration due to the formation of cross-links was expected. However, a significant decrease in DNA migration was noted only at doses of 12.2 μM or higher. This is at least twice the IC_{50} value of the drug in these cells, and a highly phototoxic dose. In the dark, **1** had no effect on DNA migration except at the highest dose (24.4 μM).

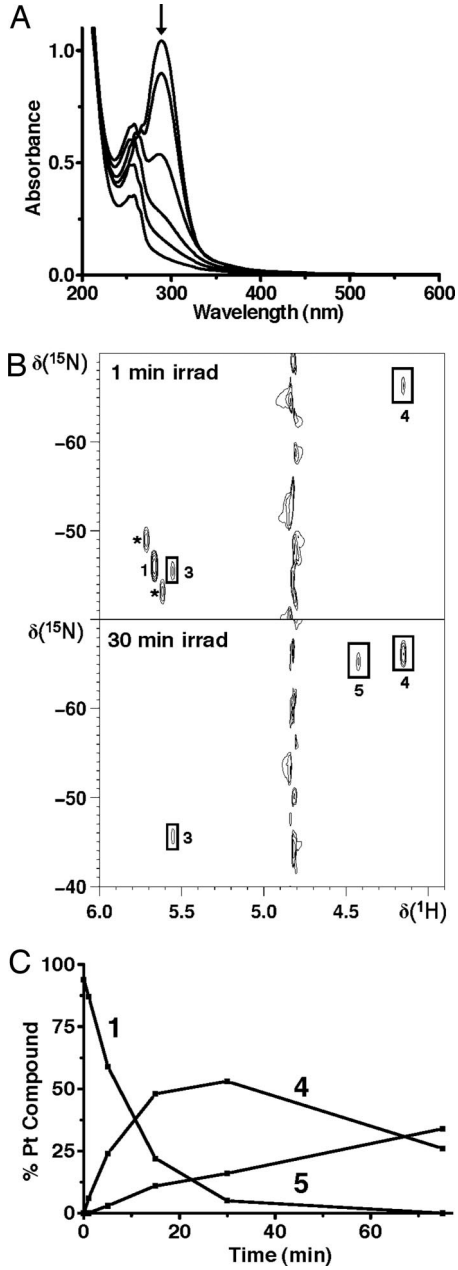

Fig. 2. Photoreactions of **1**. (*A*) UV-visible spectra recorded after 0, 1, 5, 15, 30, and 60 min of UVA irradiation. (*B*) Two-dimensional [^{1}H,^{15}N] HSQC NMR spectra for ^{15}N-**1** and 2 mol equiv 5′-GMP after 1 and 30 min of irradiation. *, ^{195}Pt satellites. (*C*) Decrease in concentration of **1** and formation of **4** and **5** with increasing irradiation time.

Caspase Activity. The concentration of **1** used in these experiments was determined from the dose-response plots of phototoxicity and produced ≈10%, 50% and 90% cell-kill 24 h after irradiation. Caspase 3 and 7 activity could not be detected by the Caspase-Glo assay either immediately after photoactivation of **1**, or 24 h after (corresponding to neutral red assay time point; SI Fig. 10). In contrast, cisplatin treatment resulted in an increase in luminescence corresponding to caspase activation.

PolyADP Ribose Polymerase and p53. Western blotting showed that polyADP ribose polymerase, a known substrate of caspase 3, was cleaved during treatment of A2780 cells with cisplatin, but not with photoactivated **1**. Cleavage was observed only when high

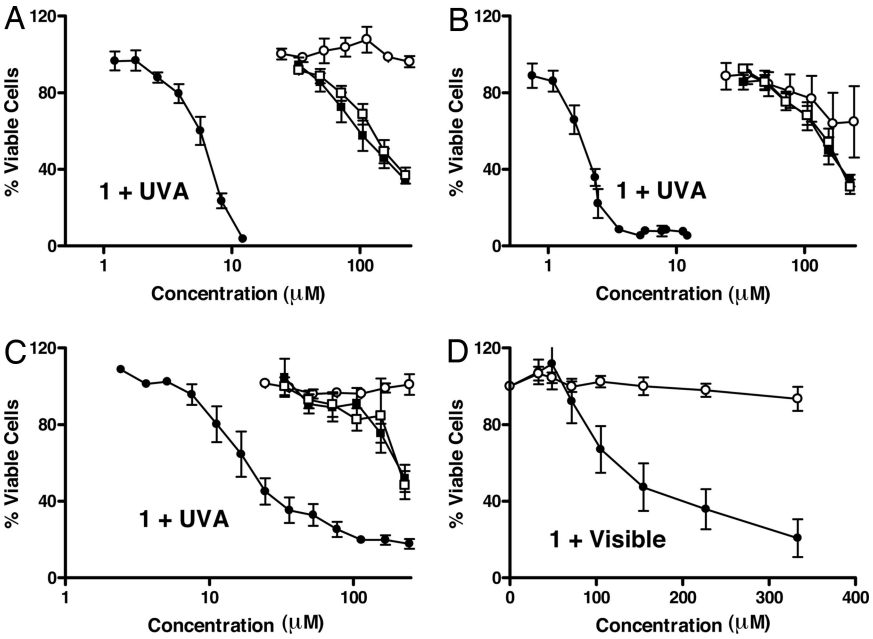

Fig. 3. Phototoxicity of complex **1**. Human HaCaT keratinocytes (*A*), A2780 human ovarian carcinoma cells (*B*), and A2780cis cisplatin-resistant cells (*C*) were exposed to 5 J/cm^2 filtered UVA or sham irradiated. (*D*) HaCaT keratinocytes exposed to 5 J/cm^2 filtered TL03 visible light (λ_{max} 420 nm). The viability of cells treated with TL03 radiation alone was 111.4%. Open symbols, sham–irradiated samples; filled symbols, irradiated samples; circles, complex **1**; squares, cisplatin.

doses of **1** were used and the cells were essentially dead (SI Fig. 11). It was evident that p53 is not detectable in cells 24 h after treatment with photoactivated **1**, in contrast to cisplatin (SI Fig. 11).

Platination of DNA in Cells. The Pt content of DNA isolated from HaCaT cells treated with 24.4 μM complex **1** and irradiated (UVA, 5 J/cm^2) was determined (by ICP-MS) to be 0.35 ± 0.05 ng Pt/μg DNA, a level similar to that after treatment with four-times higher dose of cisplatin [0.60 ± 0.39 (range 0.21–0.98) ng Pt/μg DNA; see *SI Text*].

DNA Binding. Two sets of samples of CT DNA were treated with **1**. One set was irradiated with UVA light immediately after addition of **1**, the other kept in the dark. The nonirradiated samples contained no bound Pt even after 7 h, whereas the amount of Pt bound to DNA in the irradiated samples increased with time (SI Fig. 12). After 1 min, 50% of the Pt was bound and this reached a plateau after ≈5 h of continuous irradiation (87% bound). When **1** was irradiated for 2 h and then added to DNA, the amount of bound Pt plateaued after only ≈90 min and was significantly lower (≈33%). Interestingly, when **1** was irradiated for 2 h, left in the dark for 2 h and then added to DNA, considerably less (26%) was bound to DNA even after 7 h (data not shown).

Transcription Mapping of DNA Adducts *in Vitro*. Experiments on *in vitro* RNA synthesis by T7 RNA polymerase were carried out using a linear 212-bp DNA fragment (SI Fig. 13*A*), treated with **1** (in the dark or under irradiation conditions) for 5 h. The major stop sites produced by the irradiated template treated with **1** (SI Fig. 13*B*, lane **1**Irrad) were similar to those produced by transplatin (SI Fig. 13*B*, lane Transplatin); no stop sites were produced by templates treated with **1** in the dark (SI Fig. 13*B*, lane **1**Dark). The stop sites produced by the irradiated template treated with **1** and transplatin were less regular and appeared mainly at single guanines and cytosines (i.e., at the preferential DNA binding sites of transplatin and several antitumor analogues of this Pt^{II} complex; refs. 12–14) and to a considerably less extent also at adenine sites.

Characterization of DNA Adducts. Ethidium bromide is a fluorescent probe used to characterize perturbations induced in DNA by bifunctional adducts of several Pt compounds (15, 16). The cross-links formed in double-helical DNA by a Pt complex prevent ethidium intercalation so that fluorescence is decreased in comparison with unplatinated double-helical DNA. The decrease of fluorescence caused by the adducts of photoactivated **1** was markedly more pronounced than that caused by the DNA adducts formed by cisplatin or transplatin in the dark at equivalent r_b (SI Fig. 14).

Thiourea labilizes monofunctionally bound transplatin and its analogs from DNA (17–19), whereas bifunctional adducts are resistant (17). Thiourea displaced ≈16 and 13% of photoactivated **1** from DNA after 1 and 5 h, respectively, of reaction of **1** with DNA under irradiation conditions. It can be concluded that,

Table 1. IC_{50} values (μM) of complex 1 and cisplatin with and without UVA irradiation

	IC_{50} value, μM*					
	HaCaT		A2780		A2780cis	
	365 nm	Dark	365 nm	Dark	365 nm	Dark
Complex 1	6.1 (5.6–6.6)	>244.3† (NA)	1.9 (1.7–2.0)	>244.3 (NA)	16.9 (11.7–24.7)	>244.3 (NA)
Cisplatin	144.0 (124–166)	173.3 (153–196)	151.3 (133–173)	152.0 (137–168)	261.0 (214–319)	229.0 (191–274)

NA, not applicable.

*Goodness of fit monitored by R^2 value and 95% confidence intervals (parentheses). Curves with $R^2 < 0.8$ rejected. Each value is mean of two to three independent experiments. Viability of cells treated with UVA light alone: 93.5 ± 7.6% (HaCaT); 96.1 ± 14.6% (A2780) and 84.3 ± 7.7% (A2780cis).

†> indicates IC_{50} outside concentration range used.

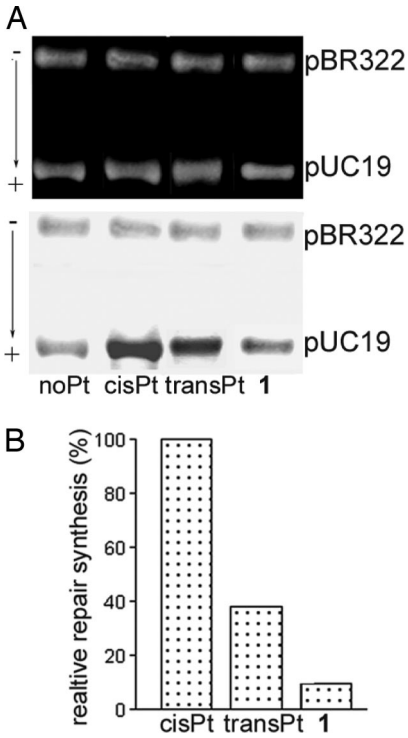

Fig. 4. *In vitro* repair synthesis assay of the extract prepared from the repair-proficient HeLa cell line. Repair synthesis used as substrates nonmodified pBR322 plasmid and pUC19 plasmid nonmodifed (lane noPt) or modified at $r_b = 0.05$ by cisplatin or transplatin in the dark (lanes cisPt and transPt, respectively), or by complex **1** under irradiation conditions (lane 1). (*A*) Results of typical experiment. (*Upper*) Photograph of the ethidium-stained gel. (*Lower*) Autoradiogram of the gel showing incorporation of [α-^{32}P]dCMP. (*B*) Incorporation of dCMP into plasmid modified by cisplatin, transplatin or complex **1**. For all quantifications, representing mean values of three separate experiments, incorporation of radioactive material was corrected for the relative DNA content in each band. Radioactivity associated with incorporation of [α-^{32}P]dCMP into DNA modified by cisplatin was taken as 100%.

at these time intervals, ≈84–87% of monofunctional adducts of photoactivated **1** had evolved to bifunctional lesions (SI Fig. 15).

DNA Interstrand Cross-Linking. The DNA interstrand cross-linking efficiency was investigated by treating a linearized plasmid pSP73 with **1**, and then irradiating or storing in the dark. The dark sample contained no bound Pt; in contrast a band corresponding to interstrand cross-linked fragments, which migrate more slowly, was seen for irradiated samples. The intensity of this band increased with increasing irradiation time. After 5 h, the frequency of interstrand CLs for **1** was 6%, compared with 4% for cisplatin and transplatin (12) (SI Fig. 16).

DNA–Protein Cross-Linking. An ability to form DNA-protein cross-links potentiates the cytotoxic effects of some antitumor Pt complexes (20). We found that photoactivation of **1** readily induces cross-links between duplex DNA (21 or 40 base pairs) and the proteins KF^- histone H1, and NF-κB (SI Fig. 17).

DNA Repair Synthesis. DNA repair synthesis by a repair-proficient HeLa CFE in a pUC19 plasmid modified by **1** and UVA light ($r_b = 0.05$), was monitored by measuring the amount of incorporated radiolabeled nucleotide. Considerably lower levels of damage-induced DNA repair synthesis were detected in the plasmid treated with **1** and UVA light in comparison to those detected in the plasmid treated with cisplatin or transplatin in the dark (Fig. 4).

Discussion

Stability and Photochemistry of 1. Complex **1** is remarkably stable in the dark, and reacted only very slowly with reduced glutathione over a period of several weeks. Such stability is important for a potential photochemotherapeutic agent, so that it can reach target sites before photoactivation. Two of the main photoproducts from irradiation of aqueous ^{15}N-**1** arose from azide substitution by hydroxide: *trans*-[$Pt^{IV}(OH)_4(^{15}NH_3)(py)$] (**2**) and *trans*-[$Pt^{IV}(N_3)(OH)_3(^{15}NH_3)(py)$] (**3**), very little reduction of Pt^{IV} to Pt^{II} was observed. However, in the presence of guanine (5′-GMP), the initial main photoproduct was the Pt^{II} monoazido species [$Pt^{II}(N_3)(^{15}NH_3)$(5′-GMP)(py)] (**4**), which suggests that the azide ligands do not leave the Pt center via a concerted mechanism. In similar reactions of the *trans* diazido diammine complex *trans*, *trans*, *trans*-[$Pt(N_3)_2(OH)_2(^{15}NH_3)_2$] with 5′-GMP (21), the analogous monoazido species (*trans*-[$Pt^{II}(N_3)(^{15}NH_3)_2$(5′-GMP)]) was not a product. This difference in photochemical behavior compared with **1** may contribute to the vastly increased phototoxic potency of **1**. The bis-5′-GMP adduct *trans*-[$Pt(^{15}NH_3)(py)$(5′-GMP)$_2]^{2+}$ (**5**) is rapidly formed from **1** upon irradiation (<5 min). The analogous complex *trans*-[$Pt(NH_3)_2$(5′-GMP)$_2]^{2+}$ is difficult to produce from reactions of transplatin under normal conditions in aqueous solution because the second hydrolysis step is very slow (22). This finding correlates with the scarcity of interstrand cross-links involving coordination of two G bases in *trans* positions for *trans* Pt^{II} diam(m)ine complexes (23), and with the inactivity of transplatin.

Phototoxicity. The neutral red phototoxicity assay has been validated against *in vivo* human reference data (24), and is designed to compare the toxicity of a drug plus light compared with either alone. The protocol prescribes a very short contact time of the cells with test compound followed by a short irradiation with a low dose of light (equivalent to ≈15–60 min on a typical U.K. midday). This is different from the constant challenge methods (typically 96 h) used to investigate cytotoxicity, but is more reflective of the conditions for use of light-activated drugs. Complex **1** rapidly accumulates in cells during the 60 min preincubation period. On photoactivation, complex **1** was much more effective at killing all three cell types than was cisplatin, but unlike cisplatin was relatively nontoxic in the dark. Encouragingly, complex **1** was 15 times more toxic to cisplatin-resistant A2780cis cells than cisplatin.

Conventional Pt-based agents, despite being among the most successful and most frequently prescribed anticancer drugs, have severe dose limiting side-effects that can result in treatment failure. Additionally, tumors can possess intrinsic resistance or acquire resistance to these drugs. A Pt prodrug that is nontoxic in the dark and activated only to the cytotoxic species when irradiated by light of the appropriate wavelength could benefit treatment outcomes and inhibit acquisition of resistance. The rapid phototoxic effect of complex **1** might arise from a number of mechanisms, including differences in the kinetics of cell uptake of the prodrug compared with cisplatin, faster kinetics of DNA reactivity of the activated complex, a different spectrum of DNA adducts formed which are more cytotoxic to the cell, and other intracellular targets that contribute to the lethal effect on photoactivation.

DNA Damage in Cells. The single-cell gel electrophoresis assay is well documented as detecting intra- and interstrand cross-links (25). HaCaT cells were treated with a clastogen immediately after the UVA-irradiation period. This produces DNA-strand breaks that result in migration of ≈70–100% of DNA from the cell nucleus. If the DNA is cross-linked, then movement is antagonized, decreasing the amount of DNA that can migrate (26). Treating cells with cisplatin or transplatin, even for a very

short time, results in the formation of DNA adducts that inhibit DNA migration in the comet assay. However, transplatin is not toxic to HaCaT or A2780 cells under our experimental conditions, nor is it therapeutically active. Thus, the technique cannot distinguish between types of cross-link unless additional enzymes are incorporated into the experimental design.

Photoactivated **1** did not replicate the activity of cisplatin when it was tested in the single-cell gel electrophoresis assay. There was limited inhibition of DNA migration. Despite this, photoactivated **1** is undoubtedly much more toxic than cisplatin; therefore, these data suggest a difference in mechanism of action.

Stabilization of p53 after genotoxic insult has also been used as a marker of DNA damage. We found that in A2780 cells, reported as having wild-type p53, the protein was stabilized and accumulated in the presence of cisplatin but not with photoactivated **1** during the time frame of our experiment.

Caspase Activity. The data suggest that cell death caused by photoactivation of **1** is not solely dependent on activation of the caspase 3 pathway. Irradiation of complex **1** did not stimulate caspase 3 activity in any of the cell lines, in contrast to cisplatin. In addition, polyADP ribose polymerase was cleaved during cisplatin treatment, but not by photoactivated **1**, unless the dose was very high. We found that the level of p53 was stabilised in the presence of cisplatin but not with photoactivated **1** (SI Fig. 11). Taken together, the cell data suggest differences in the behavior of photoactivated **1** compared with cisplatin. The complex is relatively unreactive to cells in the dark, but when irradiated it is very toxic, killing cells (including cisplatin-resistant cells), irrespective of their p53 status, by a mechanism that appears different from cisplatin.

DNA Binding and Cross-Linking. The rate of Pt binding to double-helical DNA treated with **1** and irradiated continuously by UVA was relatively high compared with the binding of nonirradiated cisplatin or transplatin (27). The binding experiments also indicate that the photoreactions result in irreversible coordination of **1** to double-helical DNA, which also facilitates sample analysis. Hence, it was possible to prepare the samples of DNA modified by **1** at a preselected value of r_b.

Platinum binding to DNA resulting from treatment of CT DNA with **1** under conditions of continuous irradiation reached a plateau after ≈5 h. However, not all Pt in the reaction mixture bound to DNA (*SI Text*). This observation might mean that the rate of binding of irradiated **1** to DNA was slower than the rate of transformation of photoactivated **1** into unreactive products. We tested this hypothesis: **1** was irradiated for 2 h and then added to DNA (see above). The results support the view that free **1** in the reaction mixture with DNA can be transformed by UVA light into species incapable of reacting with DNA.

The transcription mapping indicates that **1** binds to DNA under irradiation conditions at sites similar to those of transplatin, i.e., less regularly than cisplatin and mainly at single guanines and cytosines (i.e., at the preferential DNA binding sites of transplatin and several antitumor analogues of this Pt^{II} complex; refs. 12–14), and to a considerably less extent also at adenine sites. Considerable evidence suggests that the antitumor efficacy of bifunctional platinum compounds is the result of the formation of various types of inter- and intrastrand CLs; however, their relative efficacy remains unknown. The results of this work are consistent with the view that **1** forms on DNA under irradiation conditions only a few interstrand cross-links (≈6%). Thus, it is reasonable to suggest that photoactivated **1** forms mainly intrastrand cross-links on DNA, or possibly mainly monofunctional adducts. The monofunctional adducts of photoactivated **1** close to become bifunctional lesions with a considerably higher rate than those of transplatin (only ≈10% monofunctional adducts of transplatin incubated with DNA in the dark for 1–5 h evolve to bifunctional lesions; refs. 17 and 19). The ethidium fluorescence data suggest that the conformational distortion induced in DNA by the adducts of irradiated **1** spans more base pairs around the platination sites than the adducts of cisplatin or transplatin, presumably due to enhanced formation of more delocalized bifunctional adducts, such as 1,3-intrastrand cross-links. The latter view is also corroborated by the results of the TU experiments and by the fact that photoactivated complex **1** forms *trans* diguanine Pt^{II} adducts more readily than transplatin.

DNA Repair Synthesis. DNA adducts of photoactivated **1** induced a much lower level of repair synthesis than the adducts of transplatin or cisplatin (Fig. 4) suggesting less efficient removal from DNA and enhanced persistence of the adducts of the photoactivated **1** in comparison with the adducts of transplatin or cisplatin. Thus, one of the important factors contributing to the high cytotoxicity of photoactivated **1** appears to be a resistance of its DNA adducts to DNA repair.

Conclusions

The Pt^{IV} diazido complex *trans*, *trans*, *trans*-$[Pt(N_3)_2(OH)_2(NH_3)(py)]$ (**1**) is unreactive in the dark but a potent phototoxin when photoactivated. Photoactivated **1** forms *trans* G adducts both with model G derivatives and with plasmid DNA. DNA–protein cross-links also form readily, and DNA repair synthesis on plasmid DNA platinated by photoactivated **1** is markedly lower than for transplatin. Cell death was not solely dependent on activation of the caspase 3 pathway, and, in contrast to cisplatin, p53 protein did not accumulate in cells after photosensitization of **1**. Therefore the *trans* diazido Pt^{IV} complex **1** has an unusual mechanism of action that differs significantly from that of *cis* complexes. After the initial lack of exploration of the anticancer activity of (nonphotoactivated) *trans* Pt complexes because of the inactivity of transplatin, this is now a highly active field of research (28). It is apparent from the work described here that photoactivated *trans* Pt^{IV} complexes can exhibit remarkable cytotoxic properties. Complex **1** is a candidate for use in photoactivated cancer chemotherapy.

Materials and Methods

NMR Spectroscopy. NMR spectra were recorded at 298 K on a Bruker spectrometer (^{1}H: 500.13 MHz; ^{15}N: 50.7 MHz). Samples were prepared in 90% H_2O/10% D_2O with ^{1}H shifts referenced internally to dioxane (δ 3.764), and ^{15}N externally to $^{15}NH_4Cl$ (1 M) in HCl (1.5 M; δ 0). All data were processed with XWIN-NMR software (version 3.6, Bruker).

Photochemistry. Photoreactions of aqueous solutions of complex **1** after UVA irradiation were followed by UV-visible spectroscopy (0.05 mM) or 1D ^{1}H and 2D [^{1}H,^{15}N] HSQC NMR spectroscopy (3 mM). For the latter, the pH was adjusted to 5 with $HClO_4$, and readjusted to 5 ± 0.2 after each irradiation to ensure slow exchange of NH protons (on Pt^{IV}).

Phototoxicity. Phototoxicity was assessed using the neutral red phototoxicity assay. This is an industry standard test recommended by both the Food and Drug Administration (FDA; ref. 24) and the European Agency for the Evaluation of Medicinal Products (EMEA). The test is designed to compare the toxicity of a drug plus light, compared with the drug alone. This also reflects the conditions used for light-activated drugs. Typically, a clinical light treatment lasts for 20–60 min. Complexes were dissolved in Earle's balanced salt solution and sterile-filtered (0.22 μm) before being applied to cells. All experiments were carried out in a specially adapted photobiology laboratory, with ambient light levels <1 lux (Solatell). Cells were seeded at a density of ≈7×10^4 cells per cm^2 and left to adhere overnight. After washing cells with PBS, test compounds were added in Earle's solution and incubated for 1 h (37°C/5% CO_2). After this time, cells were irradiated (5 J cm^{-2}) with UVA. Following irradiation, the salt solution was removed, the cells thoroughly washed, and then returned to the incubator in complete growth medium. Phototoxicity was determined 24 h later using neutral red uptake (29, 30). The amount of

test compound required to inhibit dye uptake by 50% (IC_{50} value) was determined by nonlinear regression (GraphPad Prism). Experiments were performed in triplicate and each repeated two to three times, with chlorpromazine as positive control.

Single-Cell Gel Electrophoresis. Single-cell gel electrophoresis (comet assay) was performed as described in ref. 21.

Caspase Activity. Caspase activity was monitored using a luminescent Caspase-Glo 3/7 kit (Promega) according to the manufacturer's instructions.

DNA Binding. Calf thymus (CT) DNA (32 μg/ml) was incubated with **1** (8 μM) in 10 mM $NaClO_4$, 310 K. The value of r_i (molar ratio of free Pt complex to nucleotide phosphates at onset of incubation with DNA) was 0.08. Aliquots were removed at various time intervals, quickly cooled on an ice bath and then exhaustively dialyzed against 10 mM $NaClO_4$ at 277 K in the dark to remove free (unbound) Pt. The Pt content in these DNA samples (r_b) was determined by flameless atomic absorption spectroscopy. To determine whether the photoproducts which bind to DNA are stable, **1** (16 μM) was irradiated for 2 h then divided into two parts; one was added to CT DNA immediately after the irradiation, whereas the other was incubated for a further 2 h in the dark and then added to DNA. Both parts were added to the same amount of CT DNA (64 μg/ml) dissolved in 10 mM $NaClO_4$ ($r_i = 0.08$) and further incubated at 310 K in the dark for 7 h. The samples were then treated as described above.

Transcription Mapping of DNA Adducts *in Vitro*. Transcription of the (NdeI/HpaI) restriction fragment of pSP73KB DNA with DNA-dependent T7 RNA polymerase and electrophoretic analysis of transcripts were performed according to the recommended protocols (Promega Protocols and Applications, 43-46, 1989/90) and described in ref. 12.

DNA Repair Synthesis. Repair DNA synthesis of cell-free extract (CFE) was assayed using pUC19 and pBR322 plasmids. A similar amount of undamaged pBR322 of a slightly different size was included in the reactions to show the background incorporation into undamaged plasmid. This background incorporation was subtracted from that for platinated pUC19.

For details of chemicals and biochemicals, synthesis and characterization of complexes, and methods and techniques used, see *SI Text*.

ACKNOWLEDGMENTS. We thank members of COST Action D39 for stimulating discussions and Drs. Karen Harper, Steve Mason, and Lorna Eades for advice and assistance with the Cliniac linear accelerator and ICP-MS, respectively. This work was funded by Scottish Enterprise, The Wellcome Trust, Grant Agency of the Czech Republic Grants 305/05/2030 and 204/03/H016, Ministry of Health of the Czech Republic Grant NR8562-4, and Academy of Sciences of the Czech Republic Grants 1QS500040581 and KAN200200651.

1. Siddick ZH (2003) *Oncogene* 22:7265–7279.
2. Bednarski PJ, Mackay FS, Sadler PJ (2007) *Anticancer Agents Med Chem* 7:75–93.
3. Lutterman DA, Fu PK-L, Turro C (2006) *J Am Chem Soc* 128:738–739.
4. Belliston-Bittner W, Dunn AR, Nguyen YHL, Stuehr DJ, Winkler JR, Gray HB (2005) *J Am Chem Soc* 127:15907–15915.
5. Brown SB, Brown EA, Walker I (2004) *Lancet Oncol* 5:497–508.
6. Hsi RA, Rosenthal DI, Glatstein E (1999) *Drugs* 57:725–734.
7. Müller P, Schroder B, Parkinson JA, Kratochwil NA, Coxall RA, Parkin A, Parsons S, Sadler PJ (2003) *Angew Chem Int Ed* 42:335–339.
8. Bednarski PJ, Grünert R, Zielzki M, Wellner A, Mackay FS, Sadler PJ (2006) *Chem Biol* 13:61–67.
9. Kašpárková, J., Mackay FS, Brabec V, Sadler PJ (2003) *J Biol Inorg Chem* 8:741–745.
10. Chu GYH, Mansy S, Duncan RE, Tobias RS (1978) *J Am Chem Soc* 100:593–606.
11. Sigel H, Massoud NA, Corfu J (1994) *J Am Chem Soc* 116:2958–2971.
12. Brabec V, Leng M (1993) *Proc Natl Acad Sci USA* 90:5345–5349.
13. Stehlíková K, Kašpárková J, Nováková O, Martínez A, Moreno V, Brabec V (2006) *FEBS J* 273:301–314.
14. Prokop R, Kašpárková, J., Nováková, O., Marini V, Pizarro AM, Navarro-Ranninger C, Brabec V (2004) *Biochem Pharmacol* 67:1097–1109.
15. Kašpárková J, Nováková O, Vrana O, Farrell N, Brabec V (1999) *Biochemistry* 38:10997–11005.
16. Brabec V, Kašpárková J, Vrana O, Nováková O, Cox JW, Qu Y, Farrell N (1999) *Biochemistry* 38:6781–6790.
17. Eastman A, Barry MA (1987) *Biochemistry* 26:3303–3307.
18. Brabec V, Vrana O, Nováková, O., Kleinwachter V, Intini FP, Coluccia M, Natile G (1996) *Nucleic Acids Res* 24:336–341.
19. Ramos-Lima FJ, Vrana O, Quiroga AG, Navarro-Ranninger C, Halamikova A, Rybnickova H, Hejmalova L, Brabec V (2006) *J Med Chem* 49:2640–2651.
20. Chvalova K, Brabec V, Kašpárková J (2007) *Nucleic Acids Res* 35:1812–1821.
21. Mackay FS, Woods JA, Moseley H, Ferguson J, Dawson A, Parsons S, Sadler PJ (2006) *Chem Eur J* 12:3155–3161.
22. Liu Y, Intini FP, Natile G, Sletten E (2002) *J Chem Soc Dalton* 18:3489–3495.
23. Natile G, Coluccia M (2001) *Coord Chem Rev* 216–217, 383–410.
24. Spielmann H, Muller L, Averbeck D, Balls M, Brendler-Schwaab S, Castell JV, Curren, R., de Silva O, Gibbs NK, Liebsch M, *et al.* (2000) *The Second ECVAM Workshop on Phototoxicity Testing: The Report and Recommendations of ECVAM Workshop 42, ATLA* 28:777–814.
25. Hartley JM, Spanswick VJ, Gander M, Giacomini G, Whelan J, Souhami RL, Hartley JA (1999) *Clin Cancer Res* 5:507–512.
26. Almeida GM, Duarte TL, Steward WP, Jones GD (2006) *DNA Repair* 5:219–225.
27. Bancroft DP, Lepre CA, Lippard SJ (1990) *J Am Chem Soc* 112:6860–6871.
28. Farrell N (1996) in *Metal Ions in Biological Systems*, eds Sigel A, Sigel H (Dekker, New York), Vol 32, pp 603–639.
29. Borenfreund E, Puerner JA (1985) *Toxicol Lett* 24:119–124.
30. Traynor NJ, Beattie PE, Ibbotson SH, Moseley H, Ferguson J, Woods JA (2005) *Toxicol Lett* 158:220–224.